Differential Inhibition of Cytosolic PEPCK by Substrate Analogues. Kinetic and Structural Characterization of Inhibitor Recognition‡

Rose Mary Stiffin,[§,||,⊥] Sarah M. Sullivan,[§,#] Gerald M. Carlson,[||,#] and Todd Holyoak*[,#]

Department of Biochemistry and Molecular Biology, The University of Kansas Medical Center, Kansas City, Kansas 66160, and Department of Molecular Biosciences, The University of Tennessee Health Science Center, Memphis, Tennessee 38163

Received October 15, 2007; Revised Manuscript Received November 26, 2007

ABSTRACT: The mechanisms of molecular recognition of phosphoenolpyruvate (PEP) and oxaloacetate (OAA) by cytosolic phosphoenolpyruvate carboxykinase (cPEPCK) were investigated by the systematic evaluation of a variety of PEP and OAA analogues as potential reversible inhibitors of the enzyme against PEP. The molecules that inhibit the enzyme in a competitive fashion were found to fall into two general classes. Those molecules that mimic the binding geometry of PEP, namely phosphoglycolate and 3-phosphonopropionate, are found to bind weakly (millimolar K_i values). In contrast, those competitive inhibitors that mimic the binding of OAA (oxalate and phosphonoformate) coordinate directly to the active site manganese ion and bind an order of magnitude more tightly (micromolar K_i values). The competitive inhibitor sulfoacetate is found to be an outlier of these two classes, binding in a hybrid fashion utilizing modes of recognition of both PEP and OAA in order to achieve a micromolar inhibition constant in the absence of direct coordination to the active site metal. The kinetic studies in combination with the structural characterization of the five aforementioned competitive inhibitors demonstrate the molecular requirements for high affinity binding of molecules to the active site of the enzyme. These features include cis-planar carbonyl groups that are required for coordination to the active site metal, a bridging electron rich atom at the position corresponding to the C2 methylene group of OAA to facilitate interactions with R405, a carboxylate or sulfonate moiety at a position corresponding to the C1 carboxylate of OAA, and the edge-on aromatic interaction between a carboxylate and Y235.

Phosphoenolpyruvate caroxykinase (GTP) [EC 4.1.1.32] catalyzes the first committed step in gluconeogenesis. The enzyme, hereafter referred to by its acronym PEPCK,[1] converts OAA to PEP, using GTP or ITP as the phosphoryl donor. In vertebrates, PEPCK occurs as two distinct isozymes, cytosolic and mitochondrial, which are products of different genes (*1*−*3*). Both forms bind free divalent metal cations, in addition to the metal−nucleotide complex (*2*). Although these isozymes share 63% identity and possess a virtually identical three-dimensional structure (*4*−*6*), they are immunologically distinct (*2*).

In efforts to delineate the topography of the active sites of the isozymes of PEPCK, studies have been performed using analogues of PEP or OAA, either as reversible inhibitors or as alternative substrates ((*7*, *8*) and references therein). Derivatives of PEP with alkyl or halo substitutions at the third carbon, using the numbering system of Stubbe and Kenyon (*9*), have been used to demonstrate, in part, the stereospecificity of the reaction catalyzed by mPEPCK from avian liver (*10*). Studies have shown that α-hydroxyl and α-sulfhydryl carboxylic acids are poor substrates for that enzyme's phosphoryl transfer reaction (*7*).

This study systematically evaluates substrate analogues of PEP and OAA as reversible inhibitors of PEPCK when tested against PEP. With the exception of three compounds, all are bifunctional, being predominantly bicarboxylic acids, biphosphonic acids, or bisulfonic acids. Some of the bifunctional compounds are also phosphoryl or sulfonyl monocarboxylic acids. None is an amide, ester, or acyl halide because earlier studies have shown that such analogues are usually poor alternative substrates or inhibitors (*9*).

Although some of the analogues screened in this work have been used previously to study the PEP/OAA binding site of PEP-dependent enzymes (*11*−*15*) and references therein), including mPEPCK (*7*, *8*), few have been evaluated as substrate analogues of rat liver cPEPCK (*7*, *8*) and none have been structurally characterized in complex with the GTP-dependent PEPCK isozyme. Many of the compounds, such as sulfoacetate, 2,2-dimethylsulfoaceate, methanediphosphonate, and 1,2-ethanediphosphonate, have not been previously evaluated as analogues of OAA or PEP.

‡ Coordinates and structure factors have been deposited in the RCSB protein databank (http://www.rcsb.org/pdb) under the accession codes 2rk7, 2rk8, 2rka, 2rkd and 2rke.

* Corresponding author. Phone: 913-588-0795. Fax: 913-588-7440. E-mail: tholyoak@kumc.edu.

§ These authors contributed equally to the work.

|| The University of Tennessee Health Science Center.

⊥ Present address: School of Health and Natural Sciences, Florida Memorial University, 15800 NW 42nd Ave., Miami Gardens, FL 33054.

The University of Kansas Medical Center.

[1] Abbreviations: ASU, asymmetric unit; cPEPCK, cytosolic phosphoenolpyruvate carboxykinase; DTT, dithiothreitol; mPEPCK, mitochondrial phosphoenolpyruvate carboxykinase; NCS, noncrystallographic symmetry; OAA, oxaloacetic acid; PEG, polyethylene glycol; PEP, phosphoenolpyruvate; PEPC, phosphoenolpyruvate carboxylase; PEPCK, phosphoenolpyruvate carboxykinase; PGA, phosphoglycolate; RMSD, root-mean-square-deviation; TLS, translation/libration/screw.

10.1021/bi7020662 CCC: $40.75
Published on Web 01/16/2008

Table 1: Substrate Analogues of Rat Liver Cytosolic Phosphoenolpyruvate Carboxykinase

no.	name	chemical formula	% actvity remaining[a]
		Dicarboxylates	
1	oxalate[b]	$CO_2^-CO_2^-$	11[c]
2	malonate[b]	$CO_2^-CH_2CO_2^-$	102[c]
3	succinate[b]	$CO_2^-CH_2CH_2CO_2^-$	91[c]
4	sulfosuccinate[d]	$CO_2^-\mathit{C}H(SO_3^-)CH_2CO_2^-$	55[c]
5	maleate	$CO_2^-CH{:}CHCO_2^-$ (cis)	52[e]
6	fumarate	$CO_2^-CH{:}CHCO_2^-$ (trans)	83[e]
7	itaconate	$CO_2^-CH_2C(:CH_2)CO_2^-$	91[c]
8	1,2-cyclopentanedicarboxylate	$CO_2^-CH(CH_2)_3CHCO_2^-$	91[c]
9	l-aspartate[b,d]	$CO_2^-CH_2\mathit{C}H(NH_3^+)CO_2^-$	112[c]
		Phosphonyl/Phosphoryl Monocarboxylates	
10	phosphonoformate[b]	$PO_3^{2-}CO^{2-}$	12[c]
11	phosphonoacetate[b]	$PO_3^{2-}CH_2CO^{2-}$	108[c]
12	3-phosphonopropionate	$PO_3H^-CH_2CH_2CO^{2-}$	57[c]
13	phosphoglycolate[b]	$PO_3^{2-}OCH_2CO^{2-}$	25[c]
14	2-d-phosphoglycerate[b,d]	$PO_3^{2-}O\mathit{C}H(CH_2OH)CO^{2-}$	110[c]
15	2-(phosphonomethyl)acrylate[b]	$PO_3H^-CH_2C(:CH_2)CO^{2-}$	92[c]
16	6-phosphogluconate[b]	$PO_3^{2-}OCH_2(CHOH)_4CO^{2-}$	117[c]
17	*N*-phosphonomethylglycine[b]	$PO_3H^-CH_2NHCH_2CO^{2-}$	104[c]
18	2-amino-3-phosphonopropionate[d]	$PO_3H^-CH_2\mathit{C}H(NH_3^+)(CO^{2-})$	94[c]
19	2-amino-4-phosphonobutyrate[d]	$PO_3H^-(CH_2)_2\mathit{C}H(NH_3^+)(CO^{2-})$	104[c]
20	2-amino-5-phosphonovalerate[d]	$PO_3H^-(CH_2)_3\mathit{C}H(NH_3^+)CO^{2-}$	98[f]
21	serine phosphate[d]	$PO_3^{2-}OCH_2\mathit{C}H(NH_3^+)CO^{2-}$	108[f]
22	threonine phosphate[d]	$PO_3^{2-}OCH(CH_3)\mathit{C}H(NH_3^+)CO^{2-}$	97[c]
		Sulfonyl/Sulfinyl Monocarboxylates	
23	sulfoacetate	$SO_3^-CH_2CO^{2-}$	18[f]
24	2,2-dimethylsulfoacetate	$SO_3^-C(CH_3)_2CO^{2-}$	65[c]
25	3-sulfopropionate	$SO_3^-CH_2CH_2CO^{2-}$	69[c]
26	cysteic acid[d]	$SO_3^-CH_2\mathit{C}H(NH_3^+)CO^{2-}$	76[c]
27	cysteine sulfinic acid[d]	$SO_2^-CH_2\mathit{C}H(NH_3^+)CO^{2-}$	105[c]
		Diphosphoryls	
28	pyrophosphate[b]	$PO_3H^-OPO_3H^-$	22[f]
29	methanediphosphonate	$PO_3H^-CH_2PO_3H^-$	4[f]
30	1,2-ethanediphosphonate	$PO_3H^-CH_2CH_2PO_3H^-$	96[e]
		Disulfonates	
31	methanedisulfonate	$SO_3^-CH_2SO_3^-$	4[f]
32	1,2-ethanedisulfonate	$SO_3^-CH_2CH_2SO_3^-$	42[e]
		Epoxy/Aromatic Compounds	
33	phosphomycin	$CH_3CH[O]CHPO_3^{2-}$	108[c]
34	phenylphosphate[e]	$C_6H_5OPO_3^{2-}$	96[c]
35	*p*-nitrophenylphosphate	$NO_2C_6H_4OPO_3^{2-}$	103[c]

[a] In this preliminary screen, the inhibition by each compound was tested twice using two different preparations of PEPCK. The remaining percent activity listed below represents the average of the two values. [b] These compounds have been previously evaluated as either reversible inhibitors or alternative substrates for rat liver cytosolic PEPCK and other PEP-utilizing enzymes (see text for references). [c] Activity was determined at analogue and PEP concentrations of 3 mM and 40 μM, respectively. [d] For the analogues containing a chiral center, the chiral carbon is italicized. [e] Activity was determined at analogue and PEP concentrations of 6 mM and 40 μM, respectively. [f] Activity was determined at analogue and PEP concentrations of 1.5 mM and 40 μM, respectively.

The results of this study illustrate that the ability of substrate analogues to inhibit PEPCK is dependent upon their overall size and the orientation, electronic properties and charge of their functional groups. Structural characterization of the compounds bound to PEPCK demonstrates that in general there are two distinct classes of competitive inhibitors. Those mimicking PEP bind to the enzyme in an outer-sphere geometry in regard to the active site metal and have an order of magnitude lower affinity for PEPCK than those compounds mimicking the binding of OAA, found to directly coordinate to the active site metal ion. The structure−function analysis presented illustrates the mechanism of molecular recognition used by PEPCK, which can be exploited to develop novel and selective inhibitors of this important enzyme.

MATERIALS AND METHODS

Materials. The compounds used in this study are shown in Table 1, which includes their name and chemical formulas. Compounds **1**−**6**, **8**, **9**, **12**, **17**−**27**, and **29** were from Aldrich Chemicals; **14**, **15**, and **32** were from Fluka; **10**, **11**, **13**, **16**, and **33**−**35** were from Sigma; **7** and **23** were from Kodak; **28** was from Mallinckrodt; **30** was from Alfa; and **31** was from Pfaltz and Bauer. All compounds were of the highest commercially available purity. The buffers TES and HEPES were from Research Organics. DTT, PEP, IDP, and TRIS were from Sigma. OAA and NADH were from Boehringer Mannheim.

Enzymes. Malate dehydrogenase (1200 units/mg; 50% glycerol solution, v:v) was from Boerhinger Mannheim. PEPCK utilized for the kinetic studies was purified to

homogeneity from rat liver cytosol following published procedures (*16*, *17*), with the following modifications. Frozen livers from 24 h fasted male Wystar rats were purchased from Pel-Freeze. The final purification of the enzyme by affinity chromatography on agarose-adipic acid-GTP (Sigma) was performed by eluting with a NaCl step gradient (100 mM to 500 mM, in 100 mM increments) in 10 mM TES (pH 7.2), 7.5% glycerol (v:v), 0.2 mM EDTA. This procedure afforded enzyme of >95% purity, based on SDS−PAGE analysis. The enzyme preparation routinely had a specific activity of 16−24 μM of OAA formed/min/mg of protein at 25 °C. Solutions of enzyme were saturated with nitrogen and stored at 5 °C. Under these conditions, the enzyme was stable for 2−3 weeks. The concentration of PEPCK was determined spectrophotometrically, using a molar extinction coefficient of 1.15×10^5 (*16*). The enzyme utilized for the crystallographic studies was recombinantly expressed in and purified from *Escherichia coli* cells as previously described (*6*).

Inhibition Experiments. The inhibition of PEPCK by all compounds was evaluated using a continuous spectrophotometric assay in which the coupling enzyme, malate dehydrogenase, reduced OAA to malate concomitant with the oxidation of NADH to NAD^+. The decrease in absorbance at 340 nm was monitored using a Beckman DU-70 spectrophotometer equipped with a temperature controller. The standard 1 mL reaction mixture for the production of OAA contained 56 mM HEPES−KOH buffer (pH 7.0), 1 mM IDP (or alternatively, 0.1 mM GDP), 23 U malate dehydrogenase (1 unit of malate dehydrogenase is defined as 1 μmol of malate produced/min/mg of protein), 0.25 mM NADH, 2.3 mM $MnCl_2$, and 48 mM $NaHCO_3$. Under these conditions, PEP was the varied substrate. When IDP was the varied substrate for the determination of the pattern of inhibition for pyrophosphate, the fixed PEP concentration was 2 mM. Each substrate analogue solution was freshly prepared in 50 mM HEPES−KOH (pH 7.0), and these stock solutions were diluted in the same buffer, with the pH being maintained. All assay components except PEPCK were preincubated in the cuvette for 3 min at 35 °C, the standard assay temperature. This temperature was used because, during pilot experiments with the inhibitor phosphonoformate, greater inhibition was observed at 35 °C than at 20 °C. Similarly, Nowak and Mildvan (*18*) demonstrated that inhibition of yeast enolase by the PEP analogue phosphoglycolate was also temperature-dependent. In our study, the reaction was initiated by addition of enzyme (10 μL of a 0.3 μM or 1.5 μM solution diluted with 10 mM TES (pH 7.2), 0.2 mM DTT, 0.2 mM EDTA, and 7.5% glycerol (v:v)). The specific activity of enzyme in the inhibition studies is expressed as μmol of OAA formed/min/mg of protein. Assays to determine patterns of inhibition were performed in triplicate. Unless otherwise stated, titration experiments to estimate the concentration of inhibitor that caused 50% inhibition of PEPCK activity were performed in duplicate. At the highest concentrations used with PEPCK, none of the compounds evaluated in this study affected the activity of the coupling enzyme, malate dehydrogenase.

Data Analyses. The kinetic parameters for the inhibition studies were best fit to the equations for competitive inhibition (eq 1) and noncompetitive inhibition (eq 2), using the computer program and nomenclature of Cleland (*19*).

$$v = VA/[K(1+1/K_{is})+A] \quad (1)$$

$$v = VA/[K(1/K_{is})+A(1+1/K_{ii})] \quad (2)$$

The parameters are defined as follows: v is the initial velocity, V is the maximal rate of product formation in the absence of inhibitor, A is the concentration of the variable substrate, K is the apparent Michaelis constant for the varied substrate, and K_{is} and K_{ii} are the inhibition constants.

For weakly inhibitory analogues for which a complete inhibition pattern was not determined, Dixon plots were used to determine K_i values (*20*).

CRYSTALLIZATION

Crystals of PEPCK used for data collection were grown by the hanging-drop method at 25 °C by mixing 4 μL of protein [containing 10 mg/mL PEPCK, 25 mM HEPES (pH 7.5,) and 1 mM DTT] with 2 μL of mother liquor [0.1 M HEPES (pH 7.4) and 16−24% PEG 3350 and 0.5 μL of 0.1 M $MnCl_2$]. The crystals of the various inhibitor complexes were obtained and cryoprotected simultaneously by transferring the crystals to 20 μL drops containing 25% PEG 3350, 10% PEG 400, 0.1 M Hepes pH 7.5, 2 mM $MnCl_2$, and 10 mM of oxalate, PGA, phosphonoformate, phosphonopropionate, or sulfoacetate for 1 h prior to cryocooling in liquid nitrogen.

DATA COLLECTION

Data on the cryocooled crystals at −180 °C were collected using a RU-H3R rotating Cu anode X-ray generator with Blue Confocal Osmic Mirrors and a Rigaku Raxis IV++ detector. All data were integrated and scaled with HKL-2000 (*21*). Data statistics are presented in Table 2.

STRUCTURE DETERMINATION AND REFINEMENT

The new structures of the rat cytosolic enzyme were determined by molecular replacement using MOLREP (*22*) in the CCP4 (*23*) package and the previously determined structure of rat cPEPCK (PDB 2QEW (*6*)). This molecular replacement solution was refined using Refmac5 followed by manual model adjustment and rebuilding using COOT (*24*). Ligand, metal, and water addition and validation were also performed in COOT. Inspection of the $F_o - F_c$ maps indicated that in the PEPCK-Mn^{2+}-PGA structure, two conformations of bound PGA were present in each of the two molecules in the ASU. The occupancy of the two conformations was manually adjusted (0.5) to minimize positive and negative difference density peaks in the maps. The occupancy and *B*-factors for the ligands are given in Table 2.

A final round of TLS refinement was performed for all models in Refmac5. A total of 15 groups were utilized per chain in the PEPCK-Mn^{2+}-oxalate, PEPCK-Mn^{2+}-phosphonoformate, PEPCK-Mn^{2+}-phosphonopropionate, and PEPCK-Mn^{2+}-sulfoacetatate structures while 10 groups per chain were utilized in the refinement of the PEPCK-Mn^{2+}-PGA structure. The optimum TLS groups were determined by submission of the pdb files to the TLSMD server (http://skuld.bmsc.washington.edu/~tlsmd/index.html; (*25*)). In structures containing two molecules in the ASU, tight NCS

Table 2: Data and Model Statistics for the PEPCK-Mn^{2+}-oxalate, PEPCK-Mn^{2+}-phosphonoformate, PEPCK-Mn^{2+}-PGA, PEPCK-Mn^{2+}-phosphonopropionate and PEPCK-Mn^{2+}-sulfoacetate Complexes[a]

	PEPCK-Mn^{2+}-oxalate	PEPCK-Mn^{2+}-phosphonoformate	PEPCK-Mn^{2+}-PGA	PEPCK-Mn^{2+}-phosphonopropionate	PEPCK-Mn^{2+}-sulfoacetate
wavelength (Å)	1.54	1.54	1.54	1.54	1.54
space group	$P2_1$	$P2_1$	$P2_1$	$P2_1$	$P2_1$
unit cell	$a = 64.0$ Å	$a = 62.3$ Å	$a = 60.7$ Å	$a = 45.3$ Å	$a = 45.2$ Å
	$b = 118.9$ Å	$b = 119.5$ Å	$b = 119.7$ Å	$b = 119.4$ Å	$b = 119.0$ Å
	$c = 86.5$ Å	$c = 86.9$ Å	$c = 90.9$ Å	$c = 60.8$ Å	$c = 60.9$ Å
	$\alpha = \gamma = 90.0°$	$\alpha = \gamma = 90°$	$\alpha = \gamma = 90°$	$\alpha = \gamma = 90°$	$\alpha = \gamma = 90°$
	$\beta = 107.0°$	$\beta = 107.1°$	$\beta = 108.9°$	$\beta = 108.7°$	$\beta = 108.8°$
resolution limit (Å)	30.8−1.9	30.1−2.00	29.9−1.95	34.0−1.9	29.1-1.8
no. of unique reflections	91629	76020	81978	44417	50438
completeness[b] (%; all data)	99.1(93.6)	98.2 (91.1)	96.4 (93.0)	97.1 (81.3)	94.4(64.9)
redundancy[b]	5.5 (4.7)	5.7 (4.5)	6.8 (6.3)	7.0 (5.5)	8.5 (3.7)
$I/\sigma(I)$[b]	11.9(2.1)	9.7 (1.9)	16.1 (2.6)	20.2 (2.4)	19.5 (1.7)
R_{merge}[b,c]	0.09 (0.52)	0.10 (0.52)	0.07 (0.53)	0.07 (0.53)	0.08 (0.45)
no. of ASU molecules	2	2	2	1	1
solvent content (%)	40.1	39.1	38.4	39.9	39.9
R_{free}[b,d] (%)	25.6 (35.2)	24.9 (34.5)	22.2 (33.3)	23.3 (36.2)	24.9 (36.8)
R_{work}[b,e] (%)	20.7 (28.3)	19.8 (27.2)	18.5 (25.4)	18.9 (30.4)	20.5 (34.7)
average B values[f]					
protein	10.9	18.1	18.4	14.1	12.1
water	25.1	31.1	26.7	28.4	22.9
inhibitor	oxalate	phosphonoformate	PGA	phosphonopropionate	sulfoacetate
	Mol A	*Mol A*	*Mol A*	19.4	18.5
	18.0	16.4	$PGA_1 = 15.7$, oc = 0.5		
	Mol B	*Mol B*	$PGA_2 = 22.1$, oc = 0.5		
	18.6	25.0	*Mol B*		
			$PGA_1 = 14.4$, oc = 0.5		
			$PGA_2 = 19.7$, oc = 0.5		
est coord error based on max likelihood (Å)	0.125	0.143	0.115	0.122	0.118
bond length rmsd (Å)	0.009	0.008	0.008	0.008	0.009
bond angle rmsd (deg)	1.119	1.117	1.125	1.112	1.237
Ramachandran statistics (%)					
most favored	90.5	90.8	91.2	91.0	91.4
additionally allowed	8.7	8.6	8.2	8.2	7.8
generously allowed	0.6	0.3	0.6	0.8	0.8
disallowed	0.2	0.3	0	0	0

[a] Mol A, molecule A of the crystallographic dimer; Mol B, molecule B of the crystallographic dimer; oc, ligand occupancy. PGA_1 and PGA_2 correspond to the two alternate conformations of PGA present in each molecule of the PEPCK-Mn^{2+}-PGA crystallographic dimer. [b] Values in parentheses represent statistics for data in the highest-resolution shells. The highest-resolution shell comprises data in the range of 1.97−1.90, 2.07−2.00, 2.02−1.95, 1.97−1.90, and 1.85−1.80 Å for the PEPCK-Mn^{2+}-oxalate, PEPCK-Mn^{2+}-phosphonoformate, PEPCK-Mn^{2+}-PGA, PEPCK-Mn^{2+}-phosphonopropionate, and PEPCK-Mn^{2+}-sulfoacetate data sets, respectively. [c] $R_{merge} = \sum|I_{obs} - I_{avg}|/\sum I_{obs}$. [d] See Brunger (*36*) for a description of R_{free}. [e] $R_{work} = \sum||F_{obs}| - |F_{calc}||/\sum|F_{obs}|$. [f] B values indicated are residual B values after TLS refinement.

restraints were utilized during the initial rounds of refinement and were removed during the final stages of refinement. All the models have excellent stereochemistry as determined by PROCHECK (*26*). Final model statistics are presented in Table 2.

RESULTS AND DISCUSSION

Screening of Substrate Analogues. The initial preliminary screening of the compounds listed in Table 1 involved comparison of their structural similarities to OAA and PEP. One of the most important criteria in choosing compounds was that they possess functional groups similar to those of the substrates. Thus, with the exception of three compounds (**33**−**35**), the molecules screened were bifunctional (bicarboxylates, biphosphonates, or bisulfonates) or else monocarboxylates with phosphonyl or sulfonyl groups as additional anionic moieties. A second criterion was size (molecular volume and length). Bifunctional compounds with conjugated ring systems or with more than six backbone carbons were excluded. Many of the compounds evaluated have not been utilized previously, and thus represent new reversible inhibitors of rat liver cPEPCK. Inhibition was initially screened using a Dixon plot at a fixed PEP concentration of 40 μM ((1/2)K_m) and inhibitors from 1.5 to 6.0 mM. Unless otherwise stated, those analogues that caused less than 30−40% inhibition were not further studied (Table 1), although their inability to inhibit will be discussed. For the analogues that caused greater inhibition, the pattern of inhibition was determined using PEP or IDP as the varied substrate (Table 3).

Oxaloacetate Analogues as Inhibitors. Oxalate (Table 1, **1**) is a competitive inhibitor of PEPCK with a K_i of 89 μM (Table 3). This value is similar to that of the K_m for PEP (82 μM) determined under the same conditions (data not shown). In a previous study, oxalate was also found to be a competitive inhibitor with respect to OAA of the rat liver cytosolic enzyme, with a K_i equivalent to the K_m for OAA (*7*). Because of oxalate's resemblance to the enolate of pyruvate, a postulated reaction intermediate generated during the conversion of PEP to pyruvate (*27*), this analogue has been previously studied and found to be a reversible inhibitor of PEP-dependent enzymes. Crystallographic studies of PEPCK from *Anaerobiospirillum succiniciproducens* (*28*), in addition to the structure of rat PEPCK in complex with oxalate presented here, demonstrate that oxalate binds to the

Table 3: Inhibition Constant for PEP and OAA Analogues

analogue	K_i	pattern of inhibition
oxalate (**1**)	$89 \pm 4\ \mu M^a$	competitive
succinate (**3**)	>8.0 mM[b]	nd[c]
maleate (**5**)	2.0 mM[b]	nd[c]
phosphonoformate (**10**)	$230 \pm 14\ \mu M^a$	competitive
phosphoglycolate (**13**)	1.0 ± 0.04 mM[a]	competitive
3-phosphonopropionate (**12**)	1.9 ± 0.4 mM[a]	competitive
1,2-ethanediphosphonate (**30**)	5.1 ± 0.5 mM[a]	competitive
sulfoacetate (**23**)	$82.5 \pm 5\ \mu M^a$	competitive
2,2-dimethylsulfoacetate (**24**)	2.1 ± 0.2 mM[a]	competitive
3-sulfopropionate (**25**)	3.4 ± 0.3 mM[a]	competitive
sulfosuccinate (**4**)	3.3 mM[b]	nd[c]
1,2-ethanedisulfonate (**32**)	3.0 mM[b]	nd[c]
pyrophosphate (**28**)	$34 \pm 5\ \mu M^{a,d}$	noncompetitive[f]
	$64 \pm 7\ \mu M^e$	
	$172 \pm 29\ \mu M$	competitive[g]
methanediphosphonate (**29**)	$32 \pm 2\ \mu M^{a,d}$	noncompetitive
	$90 \pm 5\ \mu M^e$	
methanedisulfonate (**31**)	$27 \pm 3\ \mu M^{a,d}$	noncompetitive
	$168 \pm 25\ \mu M^e$	

[a] The K_i values were obtained using the Cleland kinetics program for competitive or noncompetitive inhibitors. [b] The K_i values were obtained from Dixon plots using two PEP concentrations. [c] Not determined. [d] Slope effect. [e] Intercept effect. [f] PEP was the varied substrate. [g] IDP was the varied substrate.

active site manganese in a bidentate fashion directly coordinating to the metal through the C1 and C2 carbonyl oxygens in an identical orientation to that of the central skeleton of the substrate OAA (Figure 1) (*6*).[2] This conformation leaves one water molecule coordinated to the active site metal, which is subsequently displaced by the γ-phosphoryl oxygen of GTP (*6*). Itaconate, the vinyl analogue of OAA, did not inhibit (Table 1, **7**), suggesting that the C3 keto oxygen present in the substrate (replaced by a methylene group in itaconic acid) is essential for the interaction of the ligand with PEPCK through direct coordination with the active site Mn^{2+} ion (*7*). Although the complete patterns of inhibition were not determined for the poor inhibitors succinate and maleate (Table 1, **3** and **5**), K_i values were obtained from Dixon plots, using two concentrations of PEP (Table 3). Succinate had a K_i value greater than 8 mM, whereas that for maleate was approximately 2 mM. Fumarate, the *trans*-isomer of maleate, did not inhibit PEPCK (Table 1, **6**). The lack of inhibition by 1,2-cyclopentanedicarboxylate (**8**) was likely due to the bulkiness of its cyclic moiety. These results are in agreement with previous findings in which putative OAA analogues were usually poor inhibitors, with K_i values above 6 mM (*7*, *29*, *30*). Taken together with the structural data, the relatively poor inhibition by the putative OAA analogues used in this and other studies demonstrates that the enzyme is relatively intolerant of changes in the bicarboxylate structure. The structure of oxalate, in combination with the lack of inhibition by itaconate and the other OAA analogues demonstrates clearly the importance of the two planar cis-carbonyl groups. The structural data demonstrate that these sp^2-hybridized centers are necessary for the cis-planar geometry (O−C−C−O torsion = −9.6°) that is required to displace the previously bound water molecules in a perfect example of entropy−entropy compensation. Further, this planar geometry is the only geometry that allows for the conjugation of the carbonyl groups and the ability to delocalize electrons through the metal center. With the exception of oxalate, all of the OAA analogues tested, while retaining a bicarboxylate electronic structure, lack this central feature and therefore would be deficient in forming the OAA-like conformation that appears to be a central motif necessary for tight binding of ligands directly to the active site manganese ion. Note the poor/lack of inhibition by malonate, maleate and succinate (Tables 1 and 3). This conclusion is further supported by previous work in which lactate, malate, nitrolactate, glycerate, thioglycolate, β-chlorolactate, and glycolate, all of which contain an sp^3-hybridized center alpha to the terminal carboxylate, are either poor substrates or poor inhibitors of mPEPCK (*7*, *8*). Additional support for this conclusion comes from the observation that only one carboxylate interacts with the active site manganese ion in the mPEPCK-Mn^{2+}-malonate-Mn^{2+}GDP structure in a geometry vastly different than that of OAA/oxalate (*5*).

While the cis-sp^2 carbonyls are necessary for micromolar inhibition, they are not the only requirement. As has been demonstrated previously, pyruvate (and its β-mercapto, fluoro, nitro, and hydroxy derivatives), glyoxylate, α-ketobutyrate, α-ketoglutarate and acetopyruvate are poor or noninhibitory compounds, despite containing the cis-sp^2-hybridized carbonyl centers (*7*, *8*). While acetopyruvate and α-ketoglutarate are likely excluded from the active site due to their large size, the other compounds are isoelectronic with OAA and would be predicted to bind more tightly than is observed based upon the above conclusion. The structural data again provide an explanation for this dramatic reduction of 100−1000-fold in binding affinity (K_i oxalate = 5−89 μM (this work and (*7*)), K_i pyruvate = 9 mM (*7*)). Comparing the tight binding analogues oxalate and phosphonoformate, it is observed that they both possess an oxygen anion that forms two short hydrogen bonds in addition to an electrostatic interaction with R405 (Figure 1). In contrast, all of the poor inhibitors mentioned above that contain the correct cis-sp^2 carbonyl structure either lack this oxygen (i.e., glyoxylate) or have a methyl or methylene center, which is incapable of taking advantage of the R405 interactions that appear to be worth between 3 and 4 kcal mol^{-1} of binding energy. As OAA contains a methylene center alpha to the sp^2 carbonyl, it raises the question of how OAA achieves the reasonable K_m of ∼2−5 μM (*7*) if the aforementioned interaction is necessary for tight binding. The structure with OAA (*6*) demonstrates that compensation for the lack of interaction between R405 and the C2 methylene group arises from interactions between R405 and/or R87 with the C1 carboxylate of OAA. Either the other inhibitors do not possess a C1 carboxylate (pyruvate and its derivatives and α-ketobutyrate) or the group is not spatially located to correctly interact in a similar fashion (α-ketoglutarate). This results in the observed poor inhibition by these molecules even in the presence of the cis carbonyl structure. This conclusion is further supported by the observation that β-sulfopyruvate is a tight binding inhibitor of mPEPCK, suggesting that the β-sulfo group effectively mimics the C1 carboxylate of OAA and therefore binds to the enzyme with a K_i similar to the K_m of OAA (K_i = 19−138 μM, (*7*)).

[2] While accepted nomenclature would indicate that the carboxylate adjacent to the keto group in OAA is the C1 carbon, in order to avoid confusion when referring to the pdb files, we have utilized the atom numbering found in the pdb description of OAA. In this description the carboxylate furthest from the keto group is numbered C1.

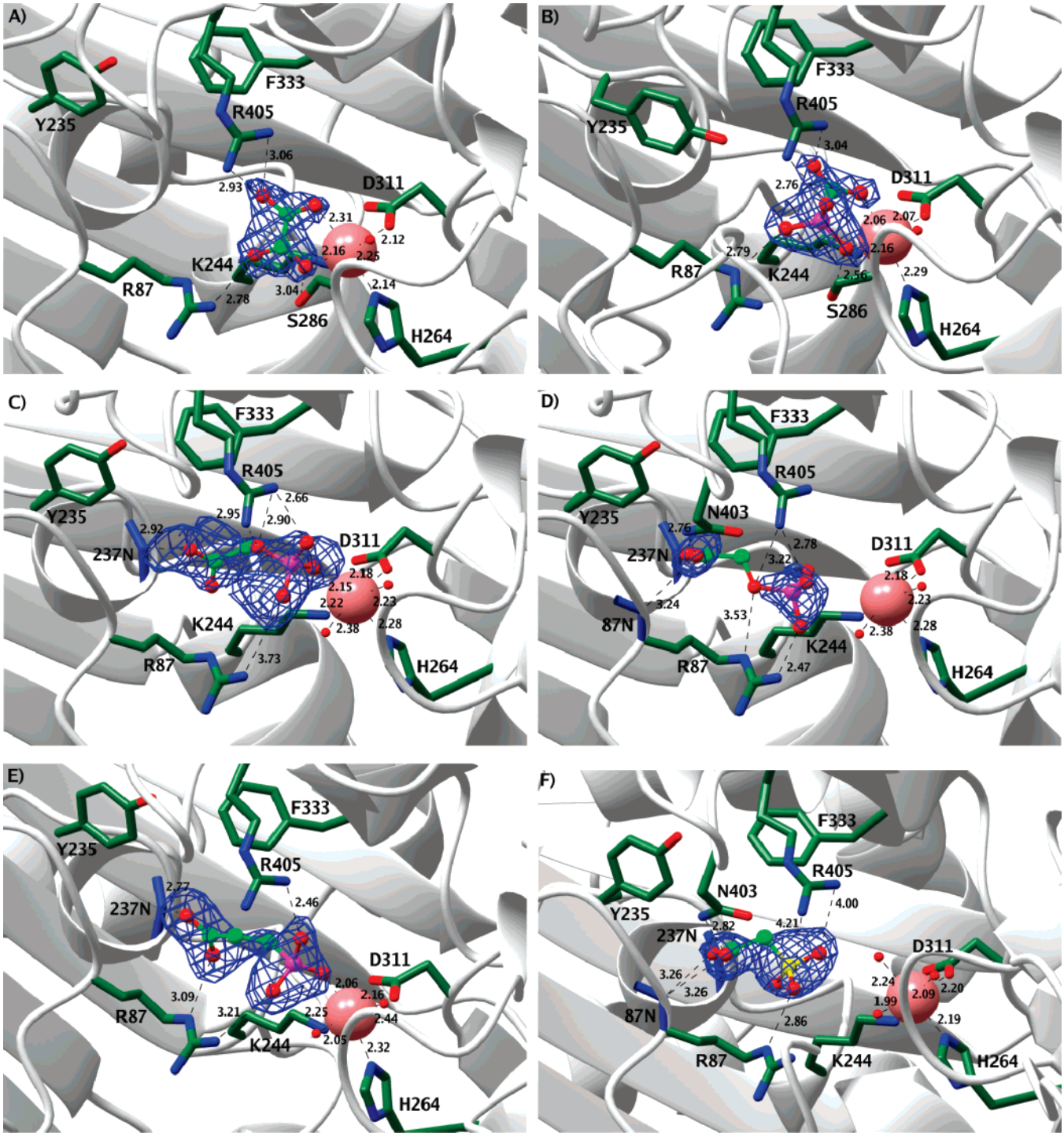

FIGURE 1: The modes of inhibitor binding to rat cPEPCK. Shown are the (A) PEPCK-Mn^{2+}-oxalate, (B) PEPCK-Mn^{2+}-phosphonoformate, (C and D) PEPCK-Mn^{2+}-PGA, (E) PEPCK-Mn^{2+}-phosphonopropionate and (F) PEPCK-Mn^{2+}-sulfoacetate complexes. The dashed lines indicate potential hydrogen bonds and metal−water interactions. In addition, a potential salt bridge between R405 and the sulfate of sulfoacetate is shown in F. All distances indicated are in angstroms. $F_o - F_c$ density rendered at (A) 2.7σ, (B) 3.3σ, (C) 2.4σ, (D) 2.4σ, (E) 3.1σ and (F) 2.8σ prior to the inclusion of the ligands into the model is shown as a blue mesh. The $F_o - F_c$ density shown in D is the residual $F_o - F_c$ density after refinement of the PGA conformation shown in C.

Phosphonoformate (Table 1, **10**) is a competitive inhibitor of PEPCK with a K_i of 231 μM (Table 3). While initially chosen as a mimic of PEP, the structural data clearly show the interaction of phosphonoformate in a mode similar to that observed for OAA (*6*) and oxalate (Figure 1). This appears to be a result of the O3 of the phosphono group and the C1 carbonyl forming the same central cis-planar oxygen geometry (O−C−P−O torsion = −14.6°) as in oxalate and OAA. In addition, consistent with the mechanism of recognition discussed above, the other carboxylate and phosphonate oxygens of phosphonoformate form similar electrostatic and hydrogen bonding interactions with R87 and R405 to those of oxalate, resulting in similar micromolar inhibition (Table 3). The slightly greater distortion from planar found in the cis carbonyl centers of phosphonoformate as compared to oxalate may explain the approximately 2-fold greater K_i observed with phosphonoformate.

Phosphoenolpyruvate Analogues as Inhibitors. Phosphoglycolate (Table 1, **13**) is a competitive inhibitor of PEPCK, with a K_i value of 1.04 mM (Table 3). Because of its marked resemblance to PEP in terms of molecular geometry, volume, and identical functional groups, this analogue has been used previously as an alternative substrate or reversible inhibitor of PEP-dependent enzymes (*15*, *18*). Not surprisingly, the structural data show a binding mode of PGA that is similar in the general orientation of the ligand to that of PEP, with the phosphate coordinating to the active site manganese ion and the ligand extending away from the ion toward Y235 (Figure 1). Unlike the other inhibitor complexes, the PGA bound to PEPCK is statically disordered and found in two different conformations in each molecule in the ASU. While one conformation is virtually identical to the bound conformation of 3-phosphonopropionate (**12**) (see below), the other conformation is unique to PGA and has the phosphate group situated in a position similar to its location in the PEPCK-Mn^{2+}-PEP complex (data not shown). As 3-phosphonopropionate is the phosphonate analogue of PGA and the two compounds are structurally similar, this additional conformation and static disorder in PGA must be due to the presence of the bridging phosphate oxygen that is absent in 3-phosphonopropionate. This conclusion is confirmed by the structural data demonstrating that the presence of the bridging phosphate oxygen atom in PGA results in the formation of a hydrogen bond with either the NH1 or NH2 group of R405 in the two bound conformations respectively. The conformation of bound inhibitor that is shared by PGA and 3-phosphonopropionate appears to be the result of the loss of the unsaturated C3 methylene group that is present in PEP. This removes an apparent aromatic interaction between the methylene group and F333 and allows the PGA and 3-phosphonopropionate inhibitors to shift in the binding pocket in a direction toward F333. This displacement in the conformation of bound PGA and 3-phosphonopropionate shown in Figure 1 results in an additional difference between the bound conformation of the inhibitors and that of PEP. While PEP is found to interact indirectly with the active site metal ion through two coordinating water molecules (*4*, *5*), one phosphate/phosphono oxygen of PGA and 3-phosphonopropionate displaces one of the metal coordinated water molecules, resulting in the phosphate/phosphono group coordinating directly to the manganese center. This change in metal coordination of the bound PGA and 3-phosphonopropionate inhibitors results in the loss of the Y235-carboxylate aromatic interaction and the hydrogen bond between the carboxylate and the side chain amide of N403 that, based upon the difference in the K_m for PEP (82 μM) and the K_i for the PGA and 3-phosphonopropionate (1−2 mM), appear to be responsible for at least 1.4 kcal mol^{-1} of binding energy.

Phosphonoacetate (**11**), a methylene homologue of phosphonoformate, is noninhibitory; however, as mentioned above, the next larger methylene homologue of phosphonoacetate, 3-phosphonopropionate (**12**), is inhibitory, with a K_i value of 1.9 mM (Table 3). The similar inhibitory capability of 3-phosphonopropionate and PGA (Table 3) is consistent with the similar size and hybridization state of the bridging methylene group and oxygen atom of the two compounds. Also, as discussed above, the structure of PEPCK in complex with 3-phosphonopropionate shows a virtually identical bound conformation to that of PGA, again consistent with their similar millimolar inhibition constants (Figure 1). Unlike what is observed with PGA versus 3-phosphonopropionate, the methylene analogue of PEP, 2-(phosphonomethyl)-acrylate, is noninhibitory (Table 1, **15**). This lack of inhibition is most likely the result of the inability of this longer inhibitor to fit within the PEP binding pocket.

2-D-Phosphoglycerate is also noninhibitory (Table 1, **14**). This analogue is similar to phosphoglycolate, except for the replacement of a C2 hydrogen with the larger $-CH_2OH$ group, whose introduction would interfere with binding at the PEP site through a steric effect. Another analogue with a bulky group at the C2 position, 2-amino-3-phosphonopropionate (**18**), likewise fails to inhibit, even though 3-phosphonopropionate is moderately inhibitory. Both 2-amino-3-phosphonopropionate and 3-phosphonopropionate also have the added negative factor of a methylene bridge between C2 and the phosphoryl group. The bridging methylene group in itself hinders binding (compare **15** with PEP); nevertheless, a negative effect of amino substitution at C2 can also be observed by comparing compounds **25** and **26**. Because the C2 carbons in 2-D-phosphoglycerate and 2-amino-3-phosphonopropionate are chiral, one might infer that the lack of inhibition could be reversed by using the L-isomer, at least in the case of phosphoglycerate. Studies have shown that the D- and L-isomers of PEP analogues inhibit some PEP-dependent enzymes differently (*12*); however, in the experiment using the noninhibitory 2-amino-3-phosphonopropionate, a racemic mixture was used. No inhibition is observed with any dicarboxylates or phosphonyl monocarboxylates that contain an amino group (Table 1, **9**, **18**−**22**), although all of these compounds are rather bulky (relatively large volumes and lengths). The analogue 6-phosphonogluconate (**16**) also does not inhibit, presumably due to its increased molecular volume and length. The lack of inhibition by these compounds illustrates the tight geometric constraints placed upon the substitution at the C2 carbon of PEP. The active site pocket for PEP is framed by R87, K244, G237, F333, R405, N403 and Y235. The structural data suggest that substitutions at C2 are limited, as these substitutions in the location of the C2 proton of PEP would sterically conflict with R87. Similarly, substitutions at the site corresponding to the C3 methylene group of PEP would seem to be limited to the native methylene group because of steric conflict with F333.

Sulfonyl Monocarboxylates as Inhibitors. A priori, these compounds were not categorized as strict OAA analogues due to the different hybridization states and geometry of their terminal groups. The carbon atom in a carboxylate anion is sp^2-hybridized, whereas the sulfur atom can be considered essentially sp^3-hybridized (*31*). The carboxylate group is planar with C_{2v} geometry, as opposed to the nonplanar C_{3v} geometry of the sulfonyl group (*32*). Although the electronic charge for both groups is the same (−1), the sulfonyl group is more electron dense. The sulfonyl monocarboxylates were not categorized as PEP analogues for similar reasons: a slight change in hybridization state (the phosphorous atom in a phosphoryl group has sp^3 hybridization and C_{3v} geometry), electron density, and a decrease of 1 in net electronic charge (*32*, *33*). As mentioned above, β-sulfopyruvate was previously reported to be a potent reversible inhibitor of avian liver mitochondrial PEPCK, with a K_i value of 7 μM (*7*).

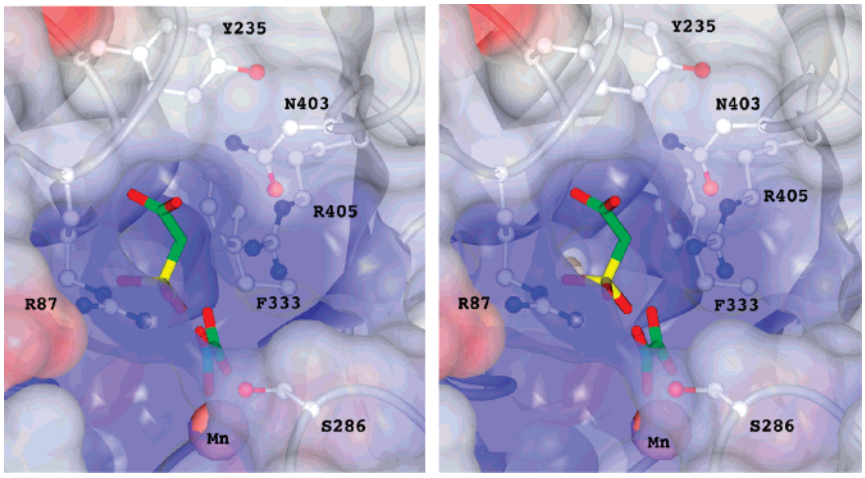

FIGURE 2: Stereoview of the OAA/PEP binding site of the lid open form of rat cPEPCK. The coloring of the protein surface was generated according to the calculated electrostatic surface potential. The coloring ranges from red (−0.5 V) to blue (+0.5 V). The electrostatic surface is rendered semitransparent illustrating the residues discussed in the text that are important for substrate recognition. These residues are labeled and rendered as white ball-and-stick-models. Bound oxalate and sulfoacetate are shown as stick models demonstrating the boundaries of the OAA/PEP binding site. The active site manganese ion is labeled and rendered as a pink sphere. For clarity, the electrostatic surface was omitted for the active site manganese ion.

The analogue was competitive with respect to OAA, with which it is isoelectronic. We have placed sulfonyl monocarboxylates in a separate class as potentially either OAA or PEP analogues, because the sulfonyl group of these compounds does not perfectly mimic either the carboxyl or phosphoryl functionalities, and thus could potentially compete with substrates for binding at either phosphoryl- or carboxyl-binding sites. However, as demonstrated by the structure of PEPCK in complex with sulfoacetate (see below), the sulfo group appears, in the case of recognition by PEPCK, to be a better analogue of the carboxylate group than the phosphate group.

Sulfoacetate (**23**) is a competitive inhibitor of PEPCK with respect to PEP, with a K_i value of 83 μM (Table 3), which is similar to the K_m value for PEP determined under these conditions. In contrast to the other micromolar inhibitors, sulfoacetate does not mimic the binding of OAA by coordinating directly to the active site metal, as would be predicted by the absence of cis-planar carbonyl groups. This inhibitor instead binds in a hybrid orientation, mimicking elements of both OAA and PEP recognition. The carboxylate of sulfoacetate binds in an identical orientation to the C1 carboxylate of PEP forming the same edge-on interaction with Y235 and a hydrogen bond between the carboxylate and N403. In contrast, the sulfo group does not mimic the binding of the phosphate of PEP; instead the sulfo group is located similarly to that of the C1 carboxylate of OAA, interacting with R87 and R405 (Figure 1). Therefore, it is apparent that the combination of the edge-on aromatic interaction and the hydrogen-bonding and electrostatic interactions with R87/405 and N403 are sufficient to result in the tight binding of the inhibitor in the absence of direct coordination to the active site manganese ion.

The analogue of sulfoacetate, 2,2-dimethylsulfoacetate (**24**), is also a competitive inhibitor, but with a K_i 25-fold greater than that of sulfoacetate (Table 3). This decrease in binding affinity is presumably due to the presence of the bulky methyl groups. 3-Sulfonopropionate (**25**) is also a poor inhibitor (Table 3), but its amino analogue cysteic acid (**26**) is even less inhibitory, whereas the related compound cysteine sulfinate (**27**) does not cause inhibition. Sulfosuccinate (**4**) is a poor inhibitor, with a K_i value of approximately 3.3 mM (Table 3); however, this inhibition is noteworthy considering that the parent compound succinate (**3**) is even less effective (Table 3). Sulfosuccinate and aspartate are both analogues of succinate, but sulfosuccinate and not aspartate (Table 1, **9**) inhibits; this difference is most likely due to the positive charge on aspartate and a negative charge on sulfosuccinate at the same carbon. These compounds also provide further evidence that the presence of an amino group on the carbon atom α to the terminal carboxyl group inhibits binding. No compound tested in this study runs counter to this observation (Table 1). These results are in agreement with a previous report that suggested that a change in the hybridization state of the C2 carbon of PEP from sp^2 to sp^3 or the incorporation of bulky groups at this position decreases affinity (*18*). Our structural data further support these observations, with the tight framing of the PEP binding pocket by F333 and R87 allowing for relatively few changes at this site of the molecule and the overall positive electrostatic potential at the active site of PEPCK (Figure 2).

Inhibition by Diphosphoryls and Diphosphonates. Pyrophosphate (**28**) is a noncompetitive inhibitor of PEPCK with respect to PEP, with a K_{is} value of 34 μM and a K_{ii} value of 63 μM. With IDP as the variable substrate, however, the inhibition pattern suggests that pyrophosphate is a competitive inhibitor (K_i of 172 μM; Table 3), perhaps competing with the α- and β-phosphates of IDP. The methylene analogue of pyrophosphate, methanediphosphonate (**29**), is also a noncompetitive inhibitor of PEPCK with respect to PEP, with inhibition constants similar to those of pyrophosphate (Table 3). This similarity in the inhibition patterns and constants observed for pyrophosphate and methanediphosphonate suggests that both compounds may bind at the same site. Although methanediphosphonate has not been previously reported as a reversible inhibitor of PEPCK from any source, or as a reversible inhibitor of any PEP-utilizing enzyme, it has been reported to be an inhibitor of pyrophosphate-dependent phosphofructokinase, with an IC_{50} of >2 mM (*34*). The homologue of methanediphosphonate, 1,2-ethanediphos-

phonate (**30**), is a poor competitive inhibitor, with a K_i value of 5.1 mM (Table 3). The functional groups on 1,2-ethanediphosphonate are in the same relative positions as those of phosphoglycolate, 3-phosphonopropionate, and 3-sulfonopropionate, each of which is a moderate to poor inhibitor of the enzyme.

The corresponding sulfonate analogues of pyrophosphonate and methanediphosphonate are pyrosulfate and methanedisulfonate (**31**). Pyrosulfate cannot be evaluated as an inhibitor because it is instantaneously converted to sulfuric acid in an aqueous environment; however, methanedisulfonate is stable and was found, like its diphosphonate analogue, to be a noncompetitive inhibitor (Table 3). The inhibition of PEPCK by pyrophosphate was anticipated, based either on its ability to chelate divalent metal cation at the active site of the metal-dependent protein or on its mimicry of the oligophosphate side chain of the nucleotide substrate (*35*). Thus, we predicted that methanediphosphonate and methanedisulfonate, being homo-bifunctional compounds of similar size and configuration as pyrophosphate, would also be noncompetitive inhibitors (Table 3, **29** and **31**). Given that the γ-phosphate of GTP acts a bridging ligand between the active site and nucleotide metals (*6*), these bifunctional compounds could be blocking the γ-phosphate's interaction with the active site metal, as this site has been crystallographically observed to bind anions such as sulfate (Holyoak and Sullivan, unpublished data). It is therefore possible that these short bifunctional compounds are bridging the two metals by binding in the γ- and β-phosphate binding site, thereby inhibiting phosphoryl transfer. The competitive inhibition of pyrophosphate against IDP is consistent with this conclusion, as the pyrophosphate and IDP are competing at least partially for the same site.

Using the double inhibition approach of Janc et al. (*14*), it was determined whether methanedisulfonate (noncompetitive inhibitor) and sulfoacetate (competitive inhibitor) could bind simultaneously to PEPCK. The parallel double inhibition patterns obtained with these two inhibitors (data not shown) are consistent with their binding being mutually exclusive. 1,2-Ethanedisulfonate (**32**), a homologue of methanedisulfonate, also inhibits, but weakly, with a K_i value of approximately 3.0 mM (Table 3). The sulfonyl groups on 1,2-ethanedisulfonate are in the same relative positions as the functional groups of the previously mentioned analogues succinate, sulfosuccinate and 1,2-ethanediphosphonate. Because all of these compounds have similar structures and are poor-to-moderate inhibitors, the decrease in affinity most likely results from their inability to mimic the bound conformation of OAA, based upon the qualities previously discussed. They are, instead, predicted to bind in a fashion similar to PEP, PGA and 3-phosphonopropionate.

A Consensus for Effective Inhibition. In general, those molecules that fail to inhibit PEPCK are predicted to be sterically prohibited from binding to the active site and/or carry positively charged functional groups incompatible with the positively charged active site (Figure 2). Of the molecules that demonstrate some affinity for the enzyme (Table 3), the structural data suggest that the phosphoryl- and phosphonomonocarboxylates attain the correct polarity in the active site via the phosphoryl/phosphono group, orienting the phosphorus containing moiety toward the manganese center and positioning the carboxylate toward the end of the pocket and Y235 and N403. These are weak inhibitors that in a general sense mimic the binding orientation of PEP; however, they appear to have a reduced edge-on carboxylate interaction with Y235 and lose the hydrogen-bonding interaction with N403 as the result of movement toward the metal and inner-sphere coordination of the phosphate to the active site manganese ion. Based upon the structures of PGA and 3-phosphonopropionate, we predict that 2,2-dimethylsulfoacetate, 1,2-ethanediphosphonate, and 3-sulfopropionate would bind in a similar outer-sphere/PEP-like conformation, resulting in their observed millimolar K_i values. It appears that PEP obtains its higher affinity for the enzyme when compared to the other PEP analogues, as represented by PGA and 3-phosphonopropionoate (89 μM vs 1−2 mM, Table 3), by taking advantage of aromatic interactions with Y235 and/or F333. Both PGA and 3-phosphonopropionate lack the C3 methylene group, which appears to make a favorable aromatic interaction with F333. This interaction also orients the carboxylate of PEP to favorably interact with Y235. The structural data suggest that the loss of the F333 interaction in PGA and 3-phosphonopropionate results in a general shift in the position of the bound inhibitor as it coordinates directly to the manganese ion, and as a result, the edge-on aromatic-carboxylate interaction with Y235 is eliminated or at least significantly decreased.

While *a priori* phosphonoformate was predicted to be a PEP analogue, the structural data demonstrate that it mimics the binding of OAA. Consistent with this observation is its micromolar K_i value similar to the K_i of oxalate. The structural data show that in phosphonoformate the juxtaposition of the two carbonyl oxygens of the phosphonate and the carboxylate allows it to mimic the planar cis-sp^2 central skeleton of OAA/oxalate, thus making it an effective analogue of OAA that binds directly to the manganese ion. Similar to oxalate, the additional interactions of the other phosphono and carboxylate oxygens with R87, S286, and R405 appear to result in the observed micomolar binding affinity.

Sulfoacetate is an outlier that utilizes motifs of both OAA and PEP recognition to achieve a reasonable binding affinity. Thus, while binding in a position similar to PEP that results in the edge-on Y235 carboxylate interaction, the sulfo group does not mimic the outer-sphere coordination of the phosphate of PEP or the inner-sphere coordination of PGA or phosphonopropionate. Instead, the sulfo group mimics the C1 carboxylate of OAA, interacting in a similar fashion with R87 and R405.

Together the kinetic and structural data suggest the following motifs for substrate/inhibitor recognition (Figure 2):

(1) Cis-planar sp^2 carbonyl moieties facilitate the coordination of the ligand directly to the active site metal. As suggested by the binding of OAA, oxalate and phosphonoformate, the terminal carbonyl should be a carboxylate in order to facilitate interaction with S286 (Figure 1) (*6*).

(2) A bridging oxygen or similar electron rich atom between the C1 carboxylate and C3 carbonyl of OAA allows for tighter binding by exploiting electrostatic and hydrogen-bonding possibilities with R405.

(3) A carboxylate or sulfonate at the position corresponding to the C1 carboxylate of OAA exploits further interactions with R87 and R405.

(4) Aromatic and hydrogen-bonding interactions at a position corresponding to the C1 carboxylate of PEP and

Y235 and N403 respectively appear to be responsible for at least an order of magnitude increase in binding efficiency.

At best, all of the molecules tested that are effective inhibitors (sulfoacetate, oxalate, and phosphonoformate) or substrates (PEP, OAA) appear to take advantage of only two of the possible interactions described above in order to achieve the observed micromolar K_i or K_m values. In theory, it should be possible to obtain quite high affinities and specificity if all four interactions are exploited, based upon the observed differences in inhibition by pyruvate and oxalate discussed previously. In addition, the binding of sulfoacetate suggests that larger molecules based upon the structure of OAA that could extend in the active site and form the favorable interactions with Y235, F333 and N403 would be potent and selective PEPCK inhibitors.

In conclusion, this study provides the first structure−function analysis of the PEP/OAA binding site of mammalian PEPCK and illustrates the mechanism of substrate/inhibitor molecular recognition utilized by PEPCK, which can be exploited in the design of effective and selective inhibitors of PEPCK.

ACKNOWLEDGMENT

We gratefully acknowledge numerous helpful comments on this work by Dr. David E. Ash (Temple University), Dr. Dennis M. Kiick (Lincoln Memorial University), Dr. Cristina T. Lewis (Genentech, Inc.), Dr. Owen W. Nadeau (University of Kansas Medical Center) and Dr. George R. Wenziger (University of South Florida). We also thank Troy Johnson (University of Kansas Medical Center) for assistance in the expression and purification of the recombinant PEPCK used in the structural studies.

REFERENCES

1. Beale, E. G., Chrapkiewicz, N. B., Scoble, H. A., Metz, R. J., Quick, D. P., Noble, R. L., Donelson, J. E., Biemann, K., and Granner, D. K. (1985) Rat hepatic cytosolic phosphoenolpyruvate carboxykinase (GTP). Structures of the protein, messenger RNA, and gene, *J. Biol. Chem. 260*, 10748−10760.
2. Utter, M. F., and Kolenbrander, H. M. (1972) in *The Enzymes* (Boyer, P. D., Ed.) pp 117−168, Academic Press, New York.
3. Weldon, S. L., Rando, A., Matathias, A. S., Hod, Y., Kalonick, P. A., Savon, S., Cook, J. S., and Hanson, R. W. (1990) Mitochondrial phosphoenolpyruvate carboxykinase from the chicken. Comparison of the cDNA and protein sequences with the cytosolic isozyme, *J. Biol. Chem. 265*, 7308−7317.
4. Dunten, P., Belunis, C., Crowther, R., Hollfelder, K., Kammlott, U., Levin, W., Michel, H., Ramsey, G. B., Swain, A., Weber, D., and Wertheimer, S. J. (2002) Crystal structure of human cytosolic phosphoenolpyruvate carboxykinase reveals a new GTP-binding site, *J. Mol. Biol. 316*, 257−264.
5. Holyoak, T., Sullivan, S. M., and Nowak, T. (2006) Structural Insights into the Mechanism of PEPCK Catalysis, *Biochemistry 45*, 8254−8263.
6. Sullivan, S. M., and Holyoak, T. (2007) Structures of rat cytosolic PEPCK: Insight into the mechanism of phosphorylation and decarboxylation of oxaloacetic acid, *Biochemistry 46*, 10078−10088.
7. Ash, D. E., Emig, F. A., Chowdhury, S. A., Satoh, Y., and Schramm, V. L. (1990) Mammalian and Avian Liver Phosphoenolpyruvate Carboxykinase−Alternate Substrates and Inhibition by Analogs of Oxaloacetate, *J. Biol. Chem. 265*, 7377−7384.
8. Guidinger, P. F., and Nowak, T. (1990) Analogs of oxalacetate as potential substrates for phosphoenolpyruvate carboxykinase, *Arch. Biochem. Biophys. 278*, 131−141.
9. Stubbe, J. A., and Kenyon, G. L. (1972) Analogs of phosphoenolpyruvate. Substrate specificities of enolase and pyruvate kinase from rabbit muscle, *Biochemistry 11*, 338−345.
10. Duffy, T. H., and Nowak, T. (1985) 1H and 31P relaxation rate studies of the interaction of phosphoenolpyruvate and its analogues with avian phosphoenolpyruvate carboxykinase, *Biochemistry 24*, 1152−1160.
11. Fitch, C. D., Chevli, R., and Jellinek, M. (1979) Phosphocreatine does not inhibit rabbit muscle phosphofructokinase or pyruvate kinase, *J. Biol. Chem. 254*, 11357−11359.
12. Izui, K., Matsuda, Y., Kameshita, I., Katsuki, H., and Woods, A. E. (1983) Phosphoenolpyruvate carboxylase of Escherichia coli. Inhibition by various analogs and homologs of phosphoenolpyruvate, *J. Biochem. (Tokyo) 94*, 1789−1795.
13. Janc, J. W., Cleland, W. W., and O'Leary, M. H. (1992) Mechanistic studies of phosphoenolpyruvate carboxylase from Zea mays utilizing formate as an alternate substrate for bicarbonate, *Biochemistry 31*, 6441−6446.
14. Janc, J. W., O'Leary, M. H., and Cleland, W. W. (1992) A kinetic investigation of phosphoenolpyruvate carboxylase from Zea mays, *Biochemistry 31*, 6421−6426.
15. Meyer, C. R., Rustin, P., and Wedding, R. T. (1989) A kinetic study of the effects of phosphate and organic phosphates on the activity of phosphoenolpyruvate carboxylase from Crassula argentea, *Arch. Biochem. Biophys. 271*, 84−97.
16. Colombo, G., Carlson, G. M., and Lardy, H. A. (1978) Phosphoenolpyruvate carboxykinase (guanosine triphosphate) from rat liver cytosol. Separation of homogeneous forms of the enzyme with high and low activity by chromatography on agarose-hexane-guanosine triphosphate, *Biochemistry 17*, 5321−5329.
17. Lewis, C. T., Seyer, J. M., and Carlson, G. M. (1989) Cysteine 288: an essential hyperreactive thiol of cytosolic phosphoenolpyruvate carboxykinase (GTP), *J. Biol. Chem. 264*, 27−33.
18. Nowak, T., and Mildvan, A. S. (1970) Stereoselective interactions of phosphoenolpyruvate analogues with phosphoenolpyruvate-utilizing enzymes, *J. Biol. Chem. 245*, 6057−6064.
19. Cleland, W. W. (1979) Statistical analysis of enzyme kinetic data, *Methods Enzymol. 63*, 103−138.
20. Segal, I. H. (1976) in *Biochemical Calculations* pp 246−273, John Wiley & Sons, New York.
21. Otwinowski, Z., and Minor, W. (1997) Processing of X-ray Diffraction Data Collected in Oscillation Mode, *Methods Enzymol. 276*, 307−326.
22. Vagin, A., and Teplyakov, A. (1997) MOLREP: an automated program for molecular replacement, *J. Appl. Crystallogr. 30*, 1022−1025.
23. Bailey, S. (1994) The Ccp4 Suite—Programs for Protein Crystallography, *Acta Crystallogr. D50*, 760−763.
24. Emsley, P., and Cowtan, K. (2004) Coot: model-building tools for molecular graphics, *Acta Crystallogr. D60*, 2126−2132.
25. Painter, J., and Merritt, E. A. (2005) A molecular viewer for the analysis of TLS rigid-body motion in macromolecules, *Acta Crystallogr. D61*, 465−471.
26. Laskowski, R. A., Macarthur, M. W., Moss, D. S., and Thornton, J. M. (1993) Procheck—a Program to Check the Stereochemical Quality of Protein Structures, *J. Appl. Crystallogr. 26*, 283−291.
27. Reed, G. H., and Morgan, S. D. (1974) Kinetic and magnetic resonance studies of the interaction of oxalate with pyruvate kinase, *Biochemistry 13*, 3537−3541.
28. Cotelesage, J. J. H., Prasad, L., Zeikus, J. G., Laivenieks, M., and Delbaere, L. T. J. (2005) Crystal structure of Anaerobiospirillum succiniciproducens PEP carboxykinase reveals an important active site loop, *Int. J. Biochem. Cell Biol. 37*, 1829.
29. Hebda, C. A., and Nowak, T. (1982) The purification, characterization, and activation of phosphoenolpyruvate carboxykinase from chicken liver mitochondria, *J. Biol. Chem. 257*, 5503−5514.
30. Hebda, C. A., and Nowak, T. (1982) Phosphoenolpyruvate carboxykinase. Mn2+ and Mn2+ substrate complexes, *J. Biol. Chem. 257*, 5515−5522.
31. Reed, A. E., and Schleyer, P. V. (1990) Chemical Bonding in Hypervalent Molecules - the Dominance of Ionic Bonding and Negative Hyperconjugation over D-Orbital Participation, *J. Am. Chem. Soc. 112*, 1434−1445.
32. Kanyo, Z. F., and Christianson, D. W. (1991) Biological recognition of phosphate and sulfate, *J. Biol. Chem. 266*, 4264−4268.
33. Radzicka, A., and Wolfenden, R. (1991) Analogues of intermediates in the action of pig kidney prolidase, *Biochemistry 30*, 4160−4164.
34. Peng, Z. Y., Mansour, J. M., Araujo, F., Ju, J. Y., McKenna, C. E., and Mansour, T. E. (1995) Some phosphonic acid analogs as

inhibitors of pyrophosphate-dependent phosphofructokinase, a novel target in Toxoplasma gondii, *Biochem. Pharmacol. 49*, 105−113.

35. Harris, W. R., and Nesset-Tollefson, D. (1991) Binding of phosphonate chelating agents and pyrophosphate to apotransferrin, *Biochemistry 30*, 6930−6936.

36. Brunger, A. T. (1992) Free R-Value - a Novel Statistical Quantity for Assessing the Accuracy of Crystal-Structures, *Nature 355*, 472−475.

BI7020662